（昭和56年11月　日本造船学会秋季講演会において講演）

A Study on Check Helms for Course Keeping of a Ship under Steady External Forces

by Shigeru Asai, *Member**

Summary

Among various aspects of manoeuvrability of ships, steerability in wind, wave, and current is one of the vitally important problems, because it is directly related to the safety of ship handling. To this steerability, rudder operations for course keeping, which are usually called as "check helms", are closely related.

Investigation was made, therefore, on a calculation method of check helms for course keeping under steady external forces. This method is derived so as to fully utilize captive model test results for assured reliability.

As an example ship form, a liquified natural gas carrier (LNGC) was examined. With the results of captive model tests, check helms and drifting angles were calculated for various design requirements which include estimation of the effects of rudder area and drifting forces due to wind and wave, together with their full-scale prediction. And it was shown that the present method is one of the practical and useful calculation methods.

1. Introduction

Under extreme environmental conditions such as high wind, rough wave, and strong current, steerability of ships becomes very important because it is directly related to the safety of navigation. Therefore, on the steerability under steady external forces, basic studies have been made by several researchers so far, especially putting an emphasis on the safety of ship operations in strong wind[1)~3)].

When a ship navigates under external disturbances due to wind, wave, etc., rudder operations for course keeping, which are usually called as "check helms", appear to be an important index for practical evaluation. Further, it will unavoidably invite drifting angles at main ship hull. These check helms and drifting angles are basic and convenient information for ship designers and ship operators to comprehend the steerability intuitively. In this study, therefore, check helms and drifting angles are adopted as expressions of important aspect of the steerability, for the sake of practical purposes.

In ship design procedure, there are growing demands for assured reliability of calculation of check helms and drifting angles under drifting forces due to wind and wave, and for confirmation of side thruster capacities. These calculations are required to include estimation of rudder area effect and prediction for full-scale ships.

Taking these situations into account, investigation is made on a calculation method of check helms and drifting angles for course keeping. This method is based on the mathematical model assured by simulation of manoeuvring motions, captive model test results, and the efficient numerical calculation technique. Calculation of check helms and drifting angles under the equilibrium conditions of total forces is called as "check helm calculation" in the present paper.

2. Mathematical Model for Manoeuvring Motions

Check helm calculation is closely related to a mathematical model for manoeuvring motions. In reference to the co-ordinate systems shown in Fig. 1, the model expressed by Eq. (1) is adopted:

$$\{\sum_{n=1}^{N}(M(j,k)-F_{a\dot{v}}(j,k))_n\}\vec{\dot{v}} = F_{\hat{v}}(j,l)_{n=1}\vec{\hat{v}}+\sum_{n=2}^{N}(\vec{F}_M(\vec{v},\vec{\delta}))_n+\vec{F}_A+\vec{F}_W \tag{1}$$

where

$M(j,k)$: Mass matrix

* Nagasaki Technical Institute, Mitsubishi Heavy Industries, Ltd.

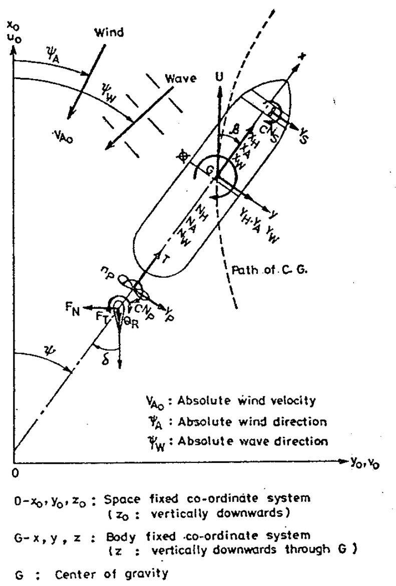

Fig. 1 System of co-ordinates

$F_{a\dot{v}}(j, k)$: Added mass matrix

$F_{\hat{v}}(j, l)$: Damping coefficient matrix

$\vec{F}_M(\vec{v}, \vec{\delta})$: Actuating force vector of manipulator

$\vec{F}_A$: Wind force vector (Suffix A denotes air.)

$\vec{F}_W$: Wave force vector (Wave drifting forces in the case of check helm calculation)

$\dot{\vec{v}}$: Acceleration vector $\dot{\vec{v}}=(\dot{u}, \dot{v}, \dot{r})$

$\vec{v}$: Velocity vector $\vec{v}=(u, v, r)$

$\hat{\vec{v}}$: Velocity vector with non-linear terms $\hat{\vec{v}}=(u, v, r, u^2, v^2, r^2, uv, vr, ru, \ldots, uvr)$; $l=(1, 2, 3, 4, 5, 6, 7, 8, 9, \ldots, 19)$

$\vec{\delta}$: Manipulating vector $\vec{\delta}=(n_P, 1, \delta, \dot{\delta}, n_S)$

j,k: Mode of motion (1: Longi. motion, 2: Sway, 3: Yaw)

N: Total number of elements of a ship form
$N=4$; for the present case
$n=1$: Main hull (H), $n=2$: Propeller (P), $n=3$: Rudder (R), $n=4$: Side thruster (S).

This model is derived on the following assumptions:

(1) Added masses of all elements (Hull: H, Propeller: P, Rudder: R, and Side thruster: S) of a ship are constant.

(2) Damping terms are attributed to a main hull and are expressed as functional forms of state variables. Damping effects of sub-elements like a propeller (P) and a rudder (R) are included in $\vec{F}_M(\vec{v}, \vec{\delta})$.

(3) Actuating forces of sub-elements P, R, and S can be correlated to their openwater characteristics through local state variables such as apparent drifting angle at the rudder position.

In the present study, important and major parameters (or functional forms) of the mathematical model are determined by captive model tests. Variation of parameters due to rudder area modification and scale effect is estimated by use of the method previously reported by the author[4].

3. Calculation Method of Check Helms

In recent trend of ship design related to check helm calculation, there have been increasing demands for full-scale prediction, estimation of rudder area effect, and effect of drifting forces due to wind and wave (wind-wave composite forces). These demands are usually followed by requirement for sufficient reliability of the calculation.

Considering these situations, a calculation method of check helms is contrived, which is composed of the mathematical model assured by simulation of manoeuvring motions and captive model test results.

To obtain a solution of equilibrium equations based on the mathematical model, two calculation methods are known so far, which can be called as "Cross curve method" and "Linearized manoeuvring indices (LMI) method". In the former,[1] advance speed U is fixed to a certain value and drifting angle β and rudder angle δ are varied stepwise. From the cross curve diagram of total forces, check helms are obtained. In the latter,[5)-7)] check helms are obtained by use of linearized manoeuvring indices through iterative procedure, flow of which is schematically explained in Appendix I.

Besides the above methods, "Multi-variable Newton (MVN) method", which is known as a numerical calculation method for a solution of multi-variable non-linear equations, can be applied. An outline of MVN method is summaried in Appendix II. The correspondence of variables and functional forms is as follows:

$$\left.\begin{array}{l} x_1=v,\ x_2=n_P,\ x_3=\delta \\ f_1=X_H+X_P+X_R+X_E \\ f_2=Y_H+Y_P+Y_R+Y_E \\ f_3=N_H+N_P+N_R+N_E \end{array}\right\} \quad (2)$$

where suffix E denotes arbitral external forces.

By use of MVN method, all sub-programs for hydrodynamic characteristics of H, P, etc., which were prepared in computing programs for manoeuvring motions, can be used as they are, because linearized derivatives are not required. And this method was checked to give solutions more rapidly than LMI method.

Stability at the equilibrium points of total forces can be evaluated by indices composed of hydrodynamic coefficients. Expressions of these indices are shown in Appendix III. In addition to this statical stability, dynamical stability is evaluated by calculation of course keeping motions under external forces as mentioned later.

4. Model Test

4.1 Tested Model

A scale model of LNGC was adopted because its steerability in wind and wave becomes often discussed. It was tested in Seakeeping and Manoeuvring Basin of Nagasaki Experimental Tank and Multi-purpose Wind Tunnel, M.H.I.

Principal particulars are shown in Table 1. Taking operation condition into account, speed of the model was adjusted to Froude's number $F_n=0.051$; with propeller revolution n_P kept at the model propulsion point.

4.2 System of Measurement

In captive model tests, total forces $(X, Y, N)_{H+P+R+S}$ acting on a hull (H) with a propeller (P), a rudder (R), and a side thruster (S) are obtained by cantilever gauges connected to the planar motion mechanism. Propeller forces $(X, Y, N)_P$ are obtained by a self-propulsion dynamometer and a propeller lateral force dynamometer. Rudder forces $(X, Y, N)_R$ are obtained by a 3-component rudder force dynamometer and side thruster forces $(Y, N)_S$ are obtained by side thruster dynamometer. Hull forces $(X, Y, N)_H$ are obtained by subtraction of P, R, S component forces from total ones.

Table 1 Principal particulars of tested ship form

Items	Model	Ship
s : Scale	1/53.200	
L_{pp} : Length between perpendiculars (m)	5.000	266.00
B : Breadth moulded (m)	0.8090	43.04
d_M : Draught moulded at midship (m)	0.2006	10.65
τ : Trim (m)	0	0
L_{pp}/B	6.180	
B/d_M	4.034	
Propeller		
D : Diameter (m)	0.1581	8.409
P : Pitch (m)	0.1097	5.838
Rudder		
Type	Mariner	
b : Breadth (m)	0.1494	7.948
h : Height (m)	0.1918	10.20
A'_{Ref} : Effective rudder area ratio	1/35.00	
Impeller of side thruster		
D_s : Diameter (m)	0.05000	2.660

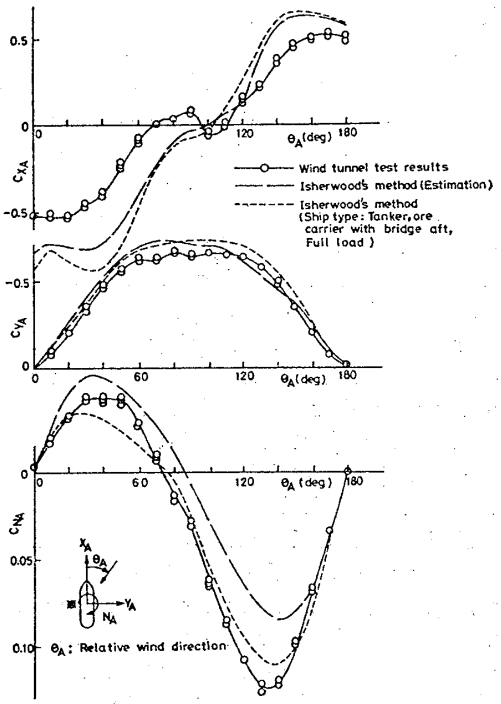

Fig. 2 Comparison of wind force coefficients

4.3 Results of Model Tests

Kinds of captive model tests are as follows:

(1) Oblique towing test
(2) Circular motion test
(3) Rudder angle test
(4) Side thruster test

In addition to the captive model tests, the following tests were carried out.

(5) Test for wave drifting force measurement
(6) Wind tunnel test

In the wind tunnel test, a water-line model (scale ratio $s=1/100$, $L_{pp}=2.66$ m) was used. Relative wind speed V_A was adjusted to 10.5 m/sec after assuring that no substantial effect of Reynolds' number is found on the range of $V_A \geqq 7.0$ m/sec. Wind forces X_A, Y_A, and N_A are non-dimensionalized by $(\rho_A/2)A_{AT}V_A^2$, $(\rho_A/2)A_{AL}V_A^2$, and $(\rho_A/2)L_{OA}A_{AL}V_A^2$ respectively, where ρ_A denotes density of air, L_{OA} length over all, A_{AT} transverse projected area above water-line and A_{AL} lateral projected area above water-line. Results of the test are shown in Fig. 2, where estimated results by Isherwood's method[8] are shown.

5. Check Helms under Steady Wind and Wave

Making use of the mathematical model together with thus obtained captive model test results, check helms are calculated of the tested ship form under steady wind and wave.

The environmental conditions for harbour entrance of the ship are prescribed as follows:

Absolute wind velocity $V_{A0} \fallingdotseq 10$ m/sec
Wave height $h_W \fallingdotseq 1.0$ m
Wave length $\lambda \fallingdotseq 66$ m ($\lambda/L \fallingdotseq 0.25$).

As for the mode of ship operations, advance speed U is regarded to be kept constant by engine control according to the operation manuals of harbour manoeuvring. Keeping of constant ship speed is realized through iterative procedure including propeller revolution n_P based on Eq. (2), and U is adjusted to relatively slow speed; i.e. $U=5$ kn ($F_n=0.051$).

5.1 Effect of Wind

Check helm calculation for the full-scale ship is made by use of wake correlation factor[9] $e_i=(1-w_m)/(1-w_s)$. The results are shown in Fig. 3, where peak value of rudder angle δ for the full-scale ship is 1.2 times larger than that for the model. As shown in Fig. 3, scale effect on the check helms is not large; therefore, hydrodynamic characteristics of the model itself are used in the following calculation.

Calculated results of the check helms under steady wind forces are shown in Fig. 4. Peak values of rudder angle δ and drifting angle β are found at relative wind direction $\theta_A=130$ and 70 degrees, respectively.

Results of the calculation on rudder area effect are shown in Fig. 5, where rudder area are varied from -30% to $+20\%$ of original one. Comparing with variation of rudder area, small variation of the check helms is found in Fig. 5. It can be said that rudder area effect on check helms is small in such a case of varied rudder area with constant rudder height as the present one.

5.2 Effect of Wave Drifting Forces

Calculated results of the check helms under steady wave drifting forces are shown in Figs. 6 and 7. Variation of the check helms with wave direction μ is shown in Fig. 6, where peak value of δ is found in the range of $\mu=50$ through 60

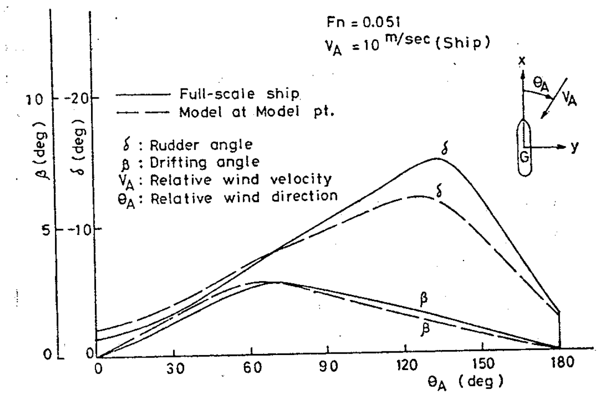

Fig. 3 Check helms and drifting angles under steady wind (Full-scale prediction)

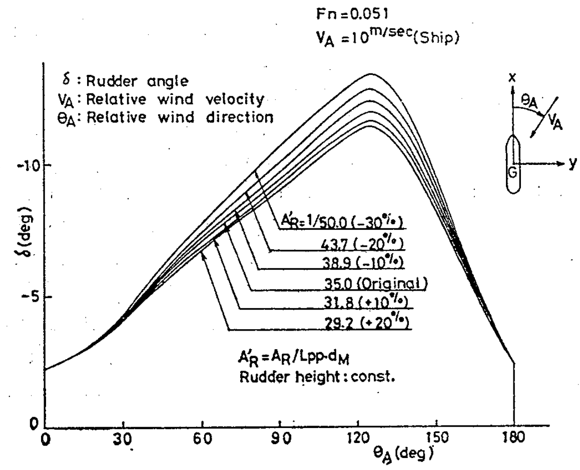

Fig. 5 Check helms under steady wind (Rudder area effect)

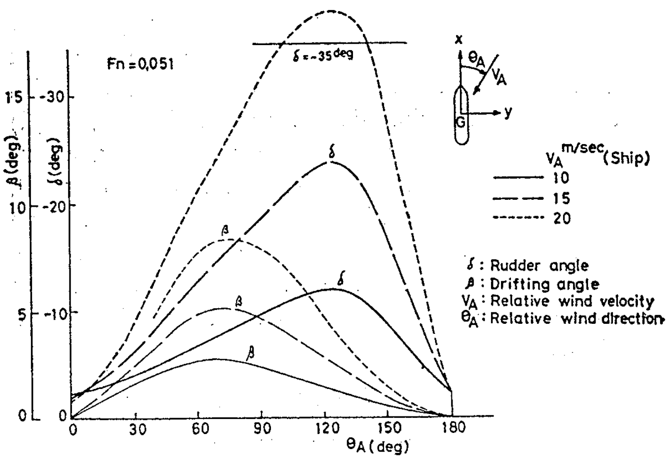

Fig. 4 Check helms and drifting angles under steady wind

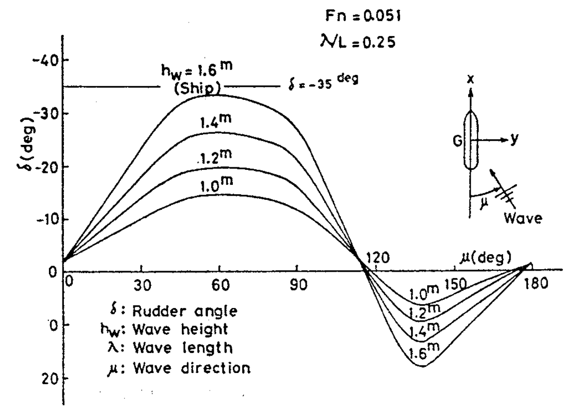

Fig. 6 Check helms under steady wave drifting forces

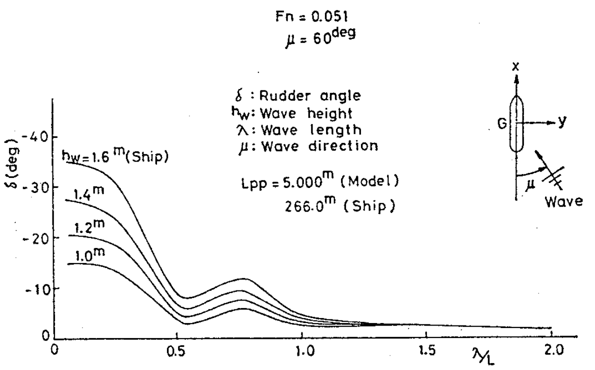

Fig. 7 Check helms under steady wave drifting forces

degrees. Variation of the check helms with wave length to ship length ratio λ/L is shown in Fig. 7, where δ markedly increases in the range of λ/L less than 0.5.

5.3 Effect of Wind-Wave Composite Forces and Side Thruster

From Figs. 4, 6 and 7, it is known that wind forces and wave drifting forces exert influences of the same order, under the design conditions of the environment. If wave drifting forces are superposed over wind forces, it is supposed that δ and β etc. become considerably large. To verify this, the severest condition; i.e. wave height $h_W=1.0$ m, $\lambda/L=0.25$, $\mu=50$ degrees, is adopted. For this condition, check helm calculation is made. The results of the calculation are shown in Fig. 8, where marked increase is noted in δ and β due to wave drifting forces. In Fig. 8, the check helms under side thruster (S/T) operation is also shown. Since the side thruster is operated to resist external yawing moment; i.e., C_{ns} is negative, where $C_{ns}=\sqrt{D_S/g}\, n_S$, δ decrease with increase of β. In the case where the side thruster is operated to resist external lateral force, increase of δ and decrease of β are confirmed by the similar calculation.

Although the effect of wind-wave composite forces on the check helms is cosiderably large, the ship form is found to have sufficient steerability because maximum check helm lies within the range of medium rudder angle.

Stability at the equilibrium points of total forces is calculated, and it is found that the equilibrium points in the range of $\theta_A \geqq 140$ degrees are unstable in the case of "Wind" when rudder angle is fixed. In the case of "Wind+Wave" and "Wind+Wave+Side thruster", every equilibrium point is statically unstable. However, a heading angle can be kept at the aimed course by the modified zig-zag manoeuvre with shifted mean value of rudder angle. Namely, the LNGC under study is dynamically stable even in wind-wave composite forces.

5.4 Effect of Water Depth

Shallow water effect becomes important under ship operations in harbours. In this study, shallow water effect on hull forces is calculated by Newman's method[10] and that on rudder forces by Kan's method[11].

Results of check helm calculation for the case of wind-wave composite forces are shown in Fig. 9, where δ and β decrease with water depth. From Fig. 9, it can be said that shallow water effect exerts more influence on β than δ.

Judging from these results summarized above, the LNGC ship form under study is considered to have satisfactory steering ability under the given environmental conditions. And it can be said that the present method of check helm calculation is practical and useful in ship design procedure.

Assuming that hydrodynamic forces due to

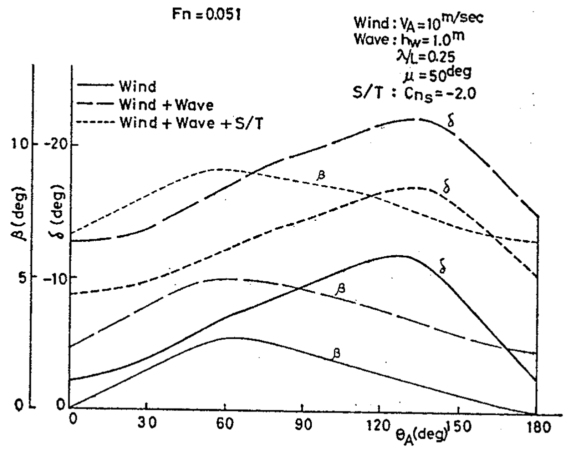

Fig. 8 Check helms and drifting angles under wind-wave composite forces and side thruster (S/T) operation

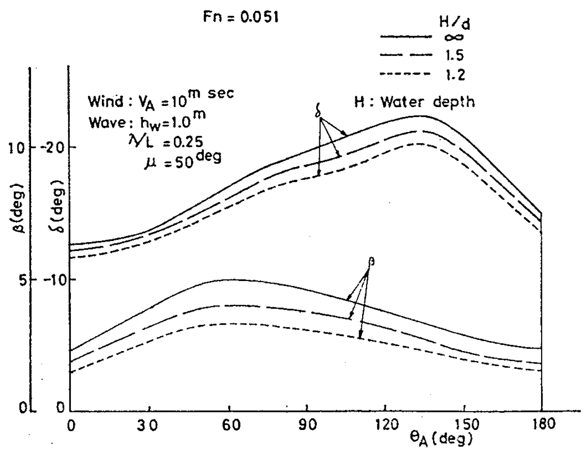

Fig. 9 Check helms and drifting angles under wind-wave composite forces (Effect of water depth)

currents can be superposed as external forces, check helms under steady currents can be also calculated by the same method as the present one.

6. Conclusions

Starting from the mathematical model, the author investigated the calculation method of check helms and drifting angles for course keeping to cope with demands in ship design.

The results of the study can be summarized as follows:

(1) A calculation method is presented, in which captive model test results are fully utilized for assured reliability.

(2) A practical example is shown of the evaluation of check helms and drifting angles by convenient expressions for ship design and navigation. And it is shown that the present method is one of the useful methods for check helm calculation.

Not only for safety, but also for minimizing ahead resistance of ships under external disturbances, such steerability calculation as the present one is considered to be increasingly important. Further study will be necessary on comparison of steerability of various ship forms.

Acknowledgement

The author wishes to express his deep appreciation to Dr. H. Fujii, Project Manager of Nagasaki Technical Institute of Mitsubishi Heavy Industries, Ltd. and to Mr. K. Tamura, Deputy General Manager of the same, and to Mr. H. Kasai, Manager of Seakeeping Research Laboratory of Nagasaki Technical Institute, for their continuing guidance and encouragement. The author also wishes to express his appreciation to Mr. Y. Watanabe, the member of Aero-Hydraulics Research Laboratory, and the members of the Seakeeping and Manoeuvring Basin of Nagasaki Technical Institute, for their cooperation in carrying out the wind tunnel test and this investigation.

References

1) A. Ogawa: Calculations on the Steered Motion of a Ship under the Action of External Forces (Part 1), J. of the Society of Naval Architects of Japan, Vol. 126 (Dec.), 1969 (in Japanese)
2) S. Inoue, et al.: The Effects of Wind on the Ship Manoeuvrability (I, II, III), Trans. of the West-Japan Society of Naval Architects, No. 44, 45, 46, (Aug. in 1972, Feb. in 1973, Aug. in 1973), (in Japanese)
3) Y. Ishibashi: On Course Stability and Manoeuvrable Range of Wind Velocity in the Uniform Wind, J. of the Society of Naval Architects of Japan, Vol. 138 (Dec.), 1975 (in Japanese)
4) S. Asai: Study on a Practical Method of Estimation for Manoeuvrability of Ships, J. of the Kansai Society of Naval Architects, No. 178 (Sept.), 1980 (in English)
5) A. Tanaka et al.: The Ship Manoeuvrability in Strong Wind, J. of the Kansai Society of Naval Architects, No. 176 (March), 1980 (in Japanese)
6) Y. Sezaki: Effects of the Wind Force to the Speed of a Car Carrier, J. of the Kansai Socity of Naval Architects, No. 179 (Dec.), 1980 (in Japanese)
7) Willem B. van Berlekom: Wind Forces on Modern Ship Forms—Effects on Performance, Advance Copy (Subject to Rivision) of North-East Coast Institution of Engineers and Shipbuilder, (Feb.), 1981 (in English), e.g.
8) R. M. Isherwood: Wind Resistance of Merchant Ships, Trans. of the Royal Institution of Naval Architects, Vol. 115, 1973 (in English)
9) H. Fujii: A Consideration on Ship-Model Correlation in Ship Manoeuvrability, Trans. of the West-Japan Society of Naval Architects, No. 62 (Aug.), 1981 (in Japanese)
10) J. N. Newman: Lateral Motion of a Slender Body between Two Parallel Walls, J. of Fluid Mechanics, Vol. 39, 1969 (in English)
11) M. Kan et al.: Analysis for the Effect of Shallow Water upon Turning, J. of the Society of Naval Architects of Japan, Vol. 115 (June), 1964 (in Japanese)

Appendix I

—Outline of Linearized Manoeuvring Indices Method—

"Linearized manoeuvring indices (LMI) method" is simply summarized by the iteration flow shown in Fig. A-I.

Appendix II

—Outline of Multi-variable Newton Method—

Multi-variable non-linear equations are expressed as follows:

$$\left.\begin{aligned} y_1 &= f_1(x_1, x_2, \cdots, x_n) \\ y_2 &= f_2(x_1, x_2, \cdots, x_n) \\ &\vdots \\ y_n &= f_n(x_1, x_2, \cdots, x_n) \end{aligned}\right\} \quad \text{(A-II-1)}$$

where the unknowns are denoted by $x_1, x_2, \ldots,$ and x_n. To solve the equation,

$$T_1(k)T_2(k)v(k,1)+(T_1(k)+T_2(k))v(k,2)+v(k,3) = K(k)(\delta_C(k)+\delta+T_3(k)\dot{\delta}+T_4^2(k)\ddot{\delta})$$

where

Mode of motion

$k=1$; Longi. motion	$v(1,1)=\ddot{u}$	$v(1,2)=\dot{u}$	$v(1,3)=u$	$\delta=\lvert\delta\rvert$
$k=2$; Sway	$v(2,1)=\ddot{v}$	$v(2,2)=\dot{v}$	$v(2,3)=v$	
$k=3$; Yaw	$v(3,1)=\ddot{r}$	$v(3,2)=\dot{r}$	$v(3,3)=r$	

$T_1(k)\cdot T_2(k) = p_v(k,1)/\ p_v(k,3)$ $T_1(k)+T_2(k) = p_v(k,2)/\ p_v(k,3)$ $T_1(k) = (p_v(k,2)+\sqrt{\lvert p_v^2(k,2)-4p_v(k,1)\cdot p_v(k,3)\rvert}\ )/(2p_v(k,3))$ $T_2(k) = (p_v(k,2)-\sqrt{\lvert p_v^2(k,2)-4p_v(k,1)\cdot p_v(k,3)\rvert}\ )/(2P_v(k,3))$
$K(k) = p_\delta(k,2)/\ p_v(k,3)$ $\delta_C(k) = p_\delta(k,1)/\ p_\delta(k,2)$ $T_3(k) = p_\delta(k,3)/\ p_\delta(k,2)$ $T_4^2(k) = p_\delta(k,4)/\ p_\delta(k,2)$
$T(k) = T_1(k)+T_2(k)-T_3(k)$ $= (p_v(k,2)\cdot p_\delta(k,2)-p_v(k,3)\cdot p_\delta(k,3)/(p_v(k,3)\cdot p_\delta(k,2))$

Table A-1 Definition of Manoeuvring Indices

$$\Sigma_{\ell=1}^{3}\{p_v(k,\ell)\cdot v(k,\ell)\} = \Sigma_{\ell=1}^{4}\{p_\delta(k,\ell)\cdot\delta(\ell)\}$$

$k=1$; Longi. motion $v(1,1)=\ddot{u}$ $v(1,2)=\dot{u}$ $v(1,3)=u$

$k=2$; Sway $v(2,1)=\ddot{v}$ $v(2,2)=\dot{v}$ $v(2,3)=v$

$k=3$; Yaw $v(3,1)=\ddot{r}$ $v(3,2)=\dot{r}$ $v(3,1)=r$

$\delta(1)=1$ $\delta(2)=\delta\ (\lvert\delta\rvert)$ $\delta(3)=\dot{\delta}\ (\lvert\dot{\delta}\rvert)$ $\delta(4)=\ddot{\delta}\ (\lvert\ddot{\delta}\rvert)$ for $k=1$

k : Mode of motion

ℓ corresponds order of differentiation.

$p_v(1,1) = 0$ $p_v(1,2) = m+m_x$ $p_v(1,3) = -X_u$	$p_\delta(1,1) = X_C+X_E$ $p_\delta(1,2) = X_{\lvert\delta\rvert}$ $p_\delta(1,3) = X_{\lvert\dot{\delta}\rvert}$ $p_\delta(1,4) = 0$
$p_v(2,1) = -(m+m_y)(Izz+Jzz)+(m_ya_y)(m_y\alpha_y)$ $p_v(2,2) = (m+m_y)N_r+(m_ya_y)\{(m+m_x)u-Y_r\}-(m_y\alpha_y)N_v+(Izz+Jzz)Y_v$ $-\frac{Y}{U}[(x_G-x_R)\{(m+m_y)N_\delta-(m_ya_y)N_\delta\}+(m_y\alpha_y)N_\delta-(Izz+Jzz)Y_\delta]$ $p_v(2,3) = -Y_vN_r-N_v\{(m+m_x)u-Y_r\}$ $+\frac{Y}{U}[(x_G-x_R)(Y_vN_\delta-N_vY_\delta)-\{(m+m_x)u-Y_r\}N_\delta-N_rY_\delta]$	$p_\delta(2,1) = \{(m+m_x)u-Y_r\}(N_C+N_E)+N_r(Y_C+Y_E)$ $-\frac{Y}{U}(x_G-x_R)\{(Y_C-Y_E)N_\delta-(N_C+N_E)Y_\delta\}$ $p_\delta(2,2) = \{(m+m_x)u-Y_r\}N_\delta+N_rY_\delta$ $p_\delta(2,3) = (m_y\alpha_y)N_\delta-(Izz+Jzz)Y_\delta+\{(m+m_x)u-Y_r\}N_{\dot{\delta}}+N_rY_{\dot{\delta}}$ $+\frac{Y}{U}(x_R-x_G)(Y_\delta N_{\dot{\delta}}-N_\delta Y_{\dot{\delta}})$ $p_\delta(2,4) = (m_y\alpha_y)N_{\dot{\delta}}-(Izz+Jzz)Y_{\dot{\delta}}$
$p_v(3,1) = -p_v(2,1)$ $p_v(3,2) = -p_v(2,2)$ $p_v(3,3) = -p_v(2,3)$	$p_\delta(3,1) = -Y_v(N_C+N_E)+N_v(Y_C+Y_E)+\frac{Y}{U}\{(Y_C+Y_E)N_\delta-(N_C+N_E)Y_\delta\}$ $p_\delta(3,2) = -Y_vN_\delta+N_vY_\delta$ $p_\delta(3,3) = (m+m_y)N_\delta-(m_ya_y)Y_\delta-Y_vN_{\dot{\delta}}+N_vY_{\dot{\delta}}-\frac{Y}{U}(Y_\delta N_{\dot{\delta}}-N_\delta Y_{\dot{\delta}})$ $p_\delta(3,4) = (m+m_y)N_{\dot{\delta}}-(m_ya_y)Y_{\dot{\delta}}$

Suffix E denotes external force due to wind, wave etc..

Table A-2 Definition of Indices p_v and p_δ

$$(y_1, y_2, \cdots, y_n)=(0, 0, 0) \tag{A-II-2}$$

let us suppose an approximate solution as follows:

$$\vec{x}=(x_1, x_2, \cdots, x_n) \tag{A-II-3}$$

an exact solution as follows:

$$\vec{x}+\Delta\vec{x}=(x_1+\Delta x_1, x_2+\Delta x_2, \cdots, x_n+\Delta x_n) \tag{A-II-4}$$

Since $\vec{x}+\Delta\vec{x}$ is an exact solution, the following equations are obtained.

$$\left.\begin{aligned} &f_1(x_1+\Delta x_1, x_2+\Delta x_2, \cdots, x_n+\Delta x_n)=0\\ &f_2(x_1+\Delta x_1, x_2+\Delta x_2, \cdots, x_n+\Delta x_n)=0\\ &\qquad\vdots\\ &f_n(x_1+\Delta x_1, x_2+\Delta x_2, \cdots, x_n+\Delta x_n)=0 \end{aligned}\right\} \tag{A-II-5}$$

By Taylor expansion of Eq. (A-II-5), the equation with first order terms is obtained as follows:

$$\left.\begin{aligned} &f_1(\vec{x})+\Delta x_1\frac{\partial f_1}{\partial x_1}(\vec{x})+\Delta x_2\frac{\partial f_1}{\partial x_2}(\vec{x})+\cdots+\Delta x_n\frac{\partial f_1}{\partial x_n}(\vec{x})=0\\ &f_2(\vec{x})+\Delta x_1\frac{\partial f_2}{\partial x_1}(\vec{x})+\Delta x_2\frac{\partial f_2}{\partial x_2}(\vec{x})+\cdots+\Delta x_n\frac{\partial f_2}{\partial x_n}(\vec{x})=0\\ &\qquad\vdots\\ &f_n(\vec{x})+\Delta x_1\frac{\partial f_n}{\partial x_1}(\vec{x})+\Delta x_2\frac{\partial f_n}{\partial x_2}(\vec{x})+\cdots+\Delta x_n\frac{\partial f_n}{\partial x_n}(\vec{x})=0 \end{aligned}\right\} \tag{A-II-6}$$

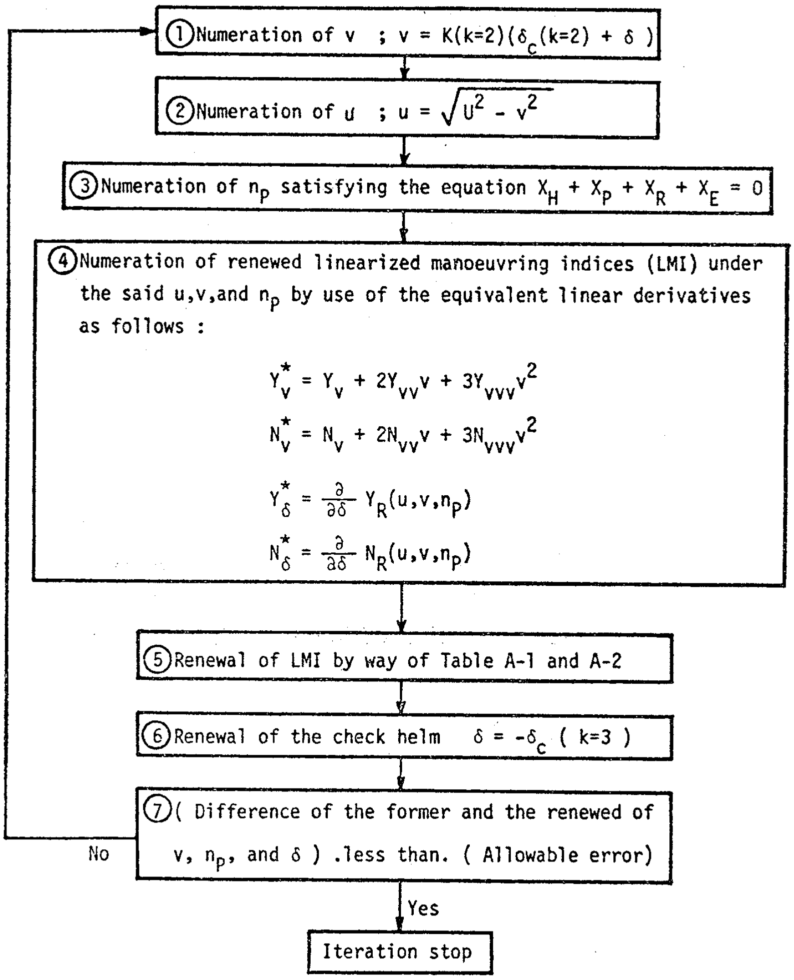

Fig. A-1 Iteration flow of LMI method

Eq. (A-II-6) can be expressed as follows:

$$\boldsymbol{A}\cdot\varDelta\vec{x}=-\vec{y} \qquad \text{(A-II-7)}$$

where

$$\boldsymbol{A}=(a_{ij}) \qquad a_{ij}=\frac{\partial f_i}{\partial x_j}(\vec{x})$$

$$\varDelta\vec{x}=\begin{bmatrix}\varDelta x_1\\ \varDelta x_2\\ \vdots\\ \varDelta x_n\end{bmatrix} \qquad \vec{y}=\begin{bmatrix}y_1\\ y_2\\ \vdots\\ y_n\end{bmatrix}$$

$\boldsymbol{A}$: Jacobian $\varDelta\vec{x}$: Correcting vector

$\vec{y}$: Residual vector.

From Eq. (A-II-7) $\varDelta x$ is obtained as follows:

$$\varDelta\vec{x}=-\vec{y}/\boldsymbol{A} \qquad \text{(A-II-8)}$$

In the practical calculation, iteration for correcting vector is made from the starting point of that $\vec{x}+\varDelta\vec{x}$ is assumed to be a renewed approximate solution.

Appendix III

—Statical Stability at Equilibrium Points—

Assuming that manipulation variables are constant, state variables are related as follows:

$$\begin{bmatrix}\dot{u}\\ \dot{v}\\ \dot{r}\\ \dot{\psi}\end{bmatrix}=\boldsymbol{A}\cdot\begin{bmatrix}u\\ v\\ r\\ \psi\end{bmatrix}, \quad \boldsymbol{A}=(a_{ij}) \qquad \text{(A-III-1)}$$

where

$$\begin{bmatrix}
a_{11}=\dfrac{\hat{X}u}{m+m_x}, & a_{12}=\dfrac{\hat{X}v}{m+m_x}, & a_{13}=\dfrac{\hat{X}r}{m+m_x}, & a_{14}=\dfrac{\hat{X}\psi\psi}{m+m_x}\\
a_{21}=\dfrac{\hat{Y}u}{m+m_y}, & a_{22}=\dfrac{\hat{Y}v}{m+m_y}, & a_{23}=\dfrac{\hat{Y}r}{m+m_y}, & a_{24}=\dfrac{\hat{Y}\psi\psi}{m+m_y}\\
a_{31}=\dfrac{\hat{N}u}{I_{zz}+J_{zz}}, & a_{32}=\dfrac{\hat{N}v}{I_{zz}+J_{zz}}, & a_{33}=\dfrac{\hat{N}r}{I_{zz}+J_{zz}}, & a_{34}=\dfrac{\hat{N}\psi\psi}{I_{zz}+J_{zz}}\\
a_{41}=0, & a_{42}=0, & a_{43}=1, & a_{44}=0
\end{bmatrix}$$

Symbol ^ atop X, Y, and N: Total forces of H, P, R, and E components

Suffix u, v, r, and ψ: Numerical differentiation at equilibrium point.

Stability of steady solutions of the above equation is evaluated by eigenvalues of matrix $\boldsymbol{A}$. The characteristics equation for these eigenvalues is expressed as follows:

$$\det(\lambda \boldsymbol{I}-\boldsymbol{A})=\lambda^4+A_3\lambda^3+A_2\lambda^2+A_1\lambda+A_0=0 \quad \text{(A-III-2)}$$

where $\boldsymbol{I}$: Unit matrix.

If the solutions of Eq. (A-III-2) have negative real part, steady solutions are stable. According to Routh–Hurwitz test, this condition is satisfied when the signs of all indices A_3, A_2, A_1, A_0, and D are the same,

where $D=A_3A_2A_1-A_3^2A_0-A_1^2$.